

## Geochemical characteristics of Recent sediments of channel bar of the Ganges (Padma) River, Bangladesh

SOHAG ALI<sup>1</sup>, MD. SHAFIQU ALAM<sup>\*1</sup>, SYED SAMSUDDIN AHMED<sup>1</sup>, MOHAMMAD NAZIM ZAMAN<sup>2</sup>, ISMAIL HOSSAIN<sup>1</sup> & PRADIP KUMAR BISWAS<sup>2</sup>

### Abstract

The present research deals with the geochemical characteristics of Recent sediments of channel bar of the Ganges (Padma) River, Bangladesh. The main objectives of the study are to delineate source area weathering, sorting and sediment recycling, provenance and tectonic setting of the Ganges sediments. The geochemical characteristics of the sediments display relatively a wide variation in accordance with lithosequences in their major element contents (e.g.  $\text{SiO}_2$ : 59.24-73.44,  $\text{Al}_2\text{O}_3$ : 10.39-15.25 in wt.%), reflecting the distinctive provenance and in part an unstable period in terms of tectonic activity. Oxides of some major elements (viz.,  $\text{K}_2\text{O}$ ,  $\text{TiO}_2$ , and  $\text{MgO}$ ) and trace elements (viz., Rb and Ni) exhibit comprehensive correlations with  $\text{Al}_2\text{O}_3$  confirming their possible hydraulic fractionation. The geochemical composition reveals that the studied sands are arkose and litharenite in type. The values of  $\text{SiO}_2/\text{Al}_2\text{O}_3$ , CIA (Chemical Index of Alteration), ICV (Index of Compositional Variability) and PIA (Plagioclase Index of Alteration) derived from the geochemical analyses of the studied sediments show low degree of maturity indicating poor chemical weathering in source areas. The entire rock geochemistry data reveals that the sediments were derived from mostly felsic to intermediate igneous rock provenance. These kinds of source rocks are present in a vast region of the Himalayan belt and catchment areas of Ganges. The tectonic setting discrimination plots ( $\text{K}_2\text{O}/\text{Na}_2\text{O}$  vs.  $\text{SiO}_2$  and  $\text{SiO}_2/\text{Al}_2\text{O}_3$  vs.  $\text{K}_2\text{O}/\text{Na}_2\text{O}$ ) shows the sediments in the source area belong to Passive Margin (PM) to Active Continental Margin (ACM).

**Keywords:** Weathering, sorting and sediment recycling, provenance and tectonic setting.

### Introduction

The Ganges River is one of the largest and most dynamic river in the world by discharge. This river begins from the Gangotri-glacier in the Himalayas, which drains through northern India and enters into Bangladesh through Chapainawabganj district in Rajshahi division of the western part of Bangladesh as the Padma River and finally, the river falls in the Bay of Bengal. The Padma is one of the largest rivers of Bangladesh, which is about 120 km long, 1.6 to 8.0 km wide and annually carries

*Authors' Addresses:* SOHAG ALI<sup>1</sup>, MD. SHAFIQU ALAM<sup>\*1</sup>, SYED SAMSUDDIN AHMED<sup>1</sup>, MOHAMMAD NAZIM ZAMAN<sup>2</sup>, ISMAIL HOSSAIN<sup>1</sup> & PRADIP KUMAR BISWAS<sup>2</sup>, <sup>1</sup>Department of Geology and Mining, University of Rajshahi, Rajshahi 6205, Bangladesh, <sup>2</sup>Institute of Mining, Mineralogy and Metallurgy (IMMM), Joypurhat, Bangladesh. E-mail: alam0809@yahoo.com.

huge amount of sediments, which are generally laid down in the beds of the river forming sand bars (ALLISON *et al.* 1998). These types of river sediments give some significant information for source rock characteristics with relief and climate, weathering, transportation and depositional mechanisms from the geochemical analysis (DICKINSON *et al.* 1983; BASU 1985; DICKINSON 1985; BHATIA 1983; TAYLOR & MCLENNAN 1985; BHATIA & CROOK 1986; ROSER & KORSCH 1986; ROSER & KORSCH 1988; MCLENNAN *et al.* 1993; CONDIE 1993; FEDO *et al.* 1995; NESBITT *et al.* 1996; CULLERS & PODKOVRV 2000; BHATT & GHOSH 2001). Moreover, several studies have been carried out focusing on the geochemical characteristics of clastic sediments as depicted by GAILLARDET *et al.* (1999), SINHA *et al.* (2007), TRIPATHI *et al.* (2007), NAJMAN *et al.* (2008), SINGH (2009, 2010), HOSSAIN *et al.* (2010), JANNATUL *et al.* (2010), GARZANTI *et al.* (2010, 2011), LUPKER *et al.* (2012), ROY & ROSER (2012), SHARMA *et al.* (2013), HOSSAIN *et al.* (2014), HAQUE *et al.* (2016), HENRY *et al.* (2017) and ABEDEN *et al.* (2018).

The present study deals with the geochemical characteristics of Recent sediments of channel bar of the Ganges (Padma) River, Bangladesh. This type of research work is still lacking in the study area though clastic sediments put up with endure a great tectonic significance. In this present research, the geochemical composition of sediments has been utilized for delineating source area weathering, sorting and sediment recycling, provenance and tectonic setting of the source rocks. This will help in comprehension of the geochemical evolution of the Himalayas as well as catchment areas of the Ganges River.

### Geological Setting

The Bengal Basin is one of the thickest sedimentary basins of the world. It stands on the eastern side of the Indian sub-continent and involves a large portion of Bangladesh and West Bengal of India and part of Bay of Bengal (ALAM 1989; HOSSAIN *et al.* 2019). It was formed during the collision of Indian and Eurasian Plate in the north and with the Burmese sub-plate in east and built the extensive Himalayan and Indo-Burman Ranges and thereby, loaded the lithosphere to form flanking sedimentary basin (UDDIN & LUNDBERG 1998; HOSSAIN *et al.* 2020).

All the rivers flow from the north to south direction because of lessening pattern of elevation from north to south. The Ganges-Padma River from the northern and western slope of the Himalayas has a catchment territory of around 907,000 sq. km. The river begins from the Gangotri-ice sheet in the Himalayas. The amount of alluvial sediments conveyed by this river is huge and the sediments contain an enormous amount of sandy materials that are generally laid down in the beds of the river forming sand bars. Geologically the study area lies in the Padma or Ganges floodplain in the southwestern part of Bogra Slope just along the northern margin of the Hinge Zone (KHAN 1991; ALAM 1992; KHAN & RAHMAN 1992; REIMANN 1993).

Geographically the study area is situated near the erosional right bank of mid channel bar of the Padma River, opposite side of Shaheed Minar Ghat, Talaimari, Rajshahi, Bangladesh which lies between latitudes  $24^{\circ} 18' 20''$  N to  $24^{\circ} 22' 48''$  N and longitudes  $88^{\circ} 30' 50''$  E to  $88^{\circ} 43' 11''$  E (Fig. 1). The geochemical analysis was carried out along the vertical lithosuccession (Fig. 3), which is located at the erosional right bank of mid channel sand bar of the Padma River.

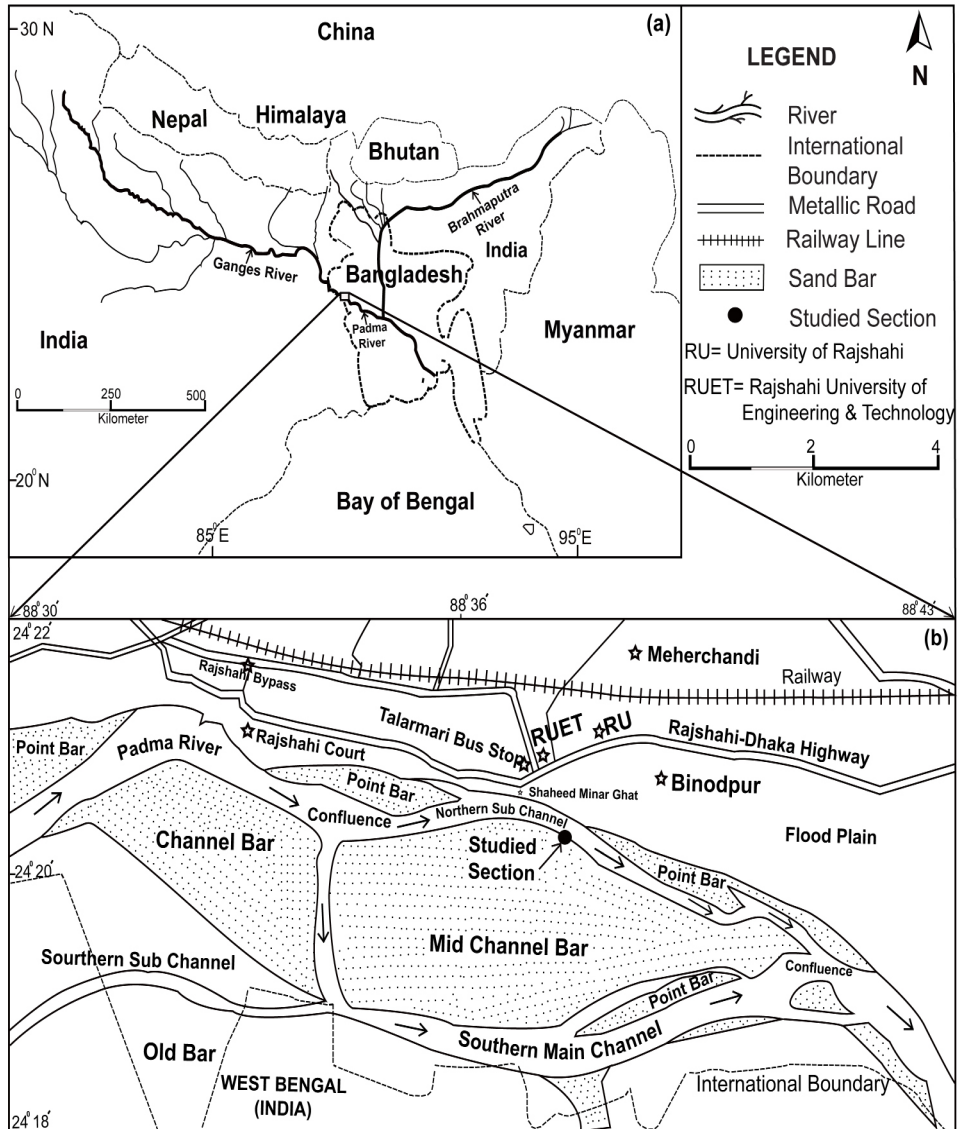


Fig. 1. Location map of the study area showing (a) the flow paths of Ganges-Padma River System and (b) geomorphic features of the Padma River (drawn after Google Earth Image).

## Methodology

The present study comprises with field and laboratory based work. A comprehensive field work was carried out along the erosional right bank of channel bar deposits of the Padma River during the dry season. During field session, some selected sections were prepared and the vertical lithosequences were studied carefully. On the basis of color, texture, bedding and different types of sedimentary structures, various types of lithofacies were identified in the study area. The thickness of each lithofacies was measured and named and coded following the facies classification schemes of MIALL (1978) and RUST (1978). A total of 23 samples were collected from different lithofacies types and depths from the vertical section. Out of the 23 samples, 12 representative samples were selected for geochemical analysis. Geochemical analysis were carried out at the Institute of Mining, Mineralogy and Metallurgy (IMMM), BCSIR, Joypurhat, Bangladesh following the procedures of GOTO & TATSUMI (1994, 1996) and also following instrumental precisions and standards described in HOSSAIN *et al.* (2014). Sample preparation techniques of the selected samples for XRF (X-Ray Fluorescence) analysis were followed according to HOSSAIN *et al.* (2014). Analytical ambiguities for XRF, major and minor elements are ~2% and trace elements are <10-15%.

Based on geochemical data, different indices and diagrams are constructed utilizing significant oxides.  $\text{CaO}^*$  exhibits the CaO in the silicate fraction merely (FEDO *et al.* 1995). The content of CaO amended for apatite utilizing  $\text{P}_2\text{O}_5$  ( $\text{CaO}^* = \text{CaO} - (10/3\text{XP}_2\text{O}_5)$ ). If the amended  $\text{CaO}^*$  was lower than the measure of  $\text{Na}_2\text{O}$ , this adjusted  $\text{CaO}^*$  value accepted. Once more, if the  $\text{CaO}^*$  value is higher than the measure of  $\text{Na}_2\text{O}$ , it was accepted that the corrected value of CaO equivalent that of  $\text{Na}_2\text{O}$ .

## Results and Discussion

### Sedimentary Lithofacies

Facies analysis of recent sedimentary sequence was carried out in a vertical section, lying at the erosional right bank of mid channel bar of the Padma River, Rajshahi, Bangladesh. The exposed section of the study area consists of predominantly sand with silt, clay, mud and plenty of root trace and organic matters. The whole section is divided into five benches (Fig. 2). The thicknesses of the benches are 2.8 m (bench-1), 1.7 m (bench-2), 1.8 m (bench-3), 2.5 m (bench-4) and 0.43 m (bench-5). Based on lithology, color, texture and different types of sedimentary structures, altogether six types of lithofacies were identified in the study area (Fig. 3). These lithofacies are planner cross stratified sand facies (Sp), ripple cross stratified sand facies (Src), ripple laminated sand facies (Sr), horizontal laminated sand facies (Sh), silt and clayey silt laminated facies (Sl) and massive mud facies (Fm). The twelve representative samples were taken from different lithofacies type for geochemical

analysis. The samples are located in the lithosequences accordingly in Fig.3.



Fig. 2. A vertical section showing different benches of the erosional right bank of mid channel bar of the Padma River, Rajshahi, Bangladesh.

### Geochemical Results

The geochemical results of XRF analysis of major oxides (in wt.%) and trace element abundances (in ppm), some calculated ratio and weathering indices from the geochemical data of the studied samples of channel bar of the Padma River, Rajshahi are presented in the Table 1.

Table 1. Major and trace elemental abundances, some ratio and weathering indices of the studied samples.

Major Oxides (wt.%)	Sample No.												Mean Value	UCC Value	PASS Value
	S-1	S-2	S-3	S-4	S-5	S-6	S-7	S-8	S-9	S-10	S-11	S-12			
SiO <sub>2</sub>	66.32	73.44	71.16	59.24	67.79	69.14	62.4	67.88	64.48	65.5	62.2	66.02	66.3	66	62.8
TiO <sub>2</sub>	0.68	0.49	0.46	0.95	0.86	0.61	0.82	0.67	0.78	0.72	0.89	0.72	0.72	0.5	1
Al <sub>2</sub> O <sub>3</sub>	11.79	10.39	10.57	15.25	11.04	12.79	13.16	11.7	13.53	13.14	13.59	11.97	12.41	15.2	18.9
Fe <sub>2</sub> O <sub>3</sub> *	7.46	4.6	4.37	8.49	6.4	5.27	8.2	7.23	6.81	6.33	8.6	7.34	6.76	4.5	6.5
MgO	2.02	1.42	1.43	2.83	1.78	2	2.38	1.45	2.36	2.18	1.8	1.61	1.94	2.2	2.2
MnO	0.1	0.07	0.07	0.11	0.11	0.08	0.11	0.09	0.09	0.09	0.11	0.1	0.09	–	–
CaO	5.58	4.27	6.23	6.56	6.38	3.71	6.46	5.25	5.81	6.04	6.57	6.3	5.76	4.2	1.3
CaO*	5.1	3.9	5.8	6	5.6	3.3	5.9	4.8	5.3	5.6	6	5.8	5.25	4.2	1.3
Na <sub>2</sub> O	1.33	1.35	1.43	0.97	1.2	1.34	1.15	0.98	1.12	1.15	0.91	0.97	1.16	3.9	1.2
K <sub>2</sub> O	3.35	3.23	3.33	4.54	3.21	4.24	4.03	3.59	3.95	4.06	4.07	3.63	3.77	3.4	3.7
P <sub>2</sub> O <sub>5</sub>	0.16	0.12	0.14	0.17	0.23	0.12	0.17	0.15	0.14	0.14	0.16	0.15	0.15	0.17	0.16
ZrO <sub>2</sub>	0.071	0.031	0.044	0.061	0.099	0.037	0.061	0.052	0.057	0.036	0.059	0.054	0.664	–	–
Trace Elements (ppm)															
Mn	740	535	511	819	882	632	821	730	689	671	866	756	721	–	–
Ba	666	432	488	782	664	525	564	500	558	697	928	754	630	550	660
Rb	207	189	187	286	184	243	253	227	236	239	268	228	229	112	160

Sr	216	186	211	239	218	183	221	210	222	225	240	224	216	350	200
Zr	528	232	329	453	731	270	455	382	424	267	440	401	409	190	210
Ni	138	74	74	326	105	78	124	136	132	101	156	140	132	20	55
Cu	64	42	49	86	54	0	77	46	70	60	78	66	58	–	–
Cr	6288	2864	2645	3668	4254	2111	5571	5299	331	2359	4990	6041	3869	35	110
Zn	80	54	56	117	74	63	93	85	96	95	97	93	84	–	–
Cl	214	332	863	396	430	429	559	282	485	395	516	529	453	–	–
F	579	0	0	0	501	1413	0	0	1343	0	0	0	320	–	–
S	62	74	125	134	91	58	97	58	86	61	68	60	81	–	–
As	24	27	0	30	0	26	27	0	0	0	30	0	14	–	–
Y	137	76	0	200	146	92	135	85	93	150	107	114	111	22	27
Mn*	0.04	0.11	0.11	0.03	0.18	0.12	0.04	0.04	0.05	0.07	0.04	0.05	0.07	–	–
Some ratios and weathering indices															
CIA*	54.8	55.2	50.1	57	52.4	59	54.3	55.7	56.5	54.9	55.3	53.5	54.94	57	75
PIA*	56.9	57.9	50.2	60.6	53.4	64.8	56.4	58.6	59.7	57.5	57.9	55.2	57.42	59	86
MIA*	9.5	10.3	0.2	14	4.8	18.1	8.5	11.3	13	9.8	10.5	7.1	9.5	10.3	0.2
ICV*	1.7	1.5	1.6	1.6	1.8	1.3	1.8	1.6	1.5	1.6	1.7	1.7	1.62	1.3	0.8
CIW*	64.9	66.6	59.5	68.6	61.8	73.4	65.1	67.1	67.7	66.1	66.2	63.9	65.95	–	–
SiO <sub>2</sub> / Al <sub>2</sub> O <sub>3</sub>	5.625	7.071	6.732	3.884	6.140	5.404	4.743	5.802	4.766	4.983	4.577	5.516	5.437	–	–
K <sub>2</sub> O / Na <sub>2</sub> O	2.52	2.4	2.33	4.69	2.69	3.16	3.5	3.67	3.52	3.53	4.47	3.73	3.35	0.87	3.1
log (SiO <sub>2</sub> / Al <sub>2</sub> O <sub>3</sub> )	0.75	0.849	0.828	0.589	0.788	0.733	0.676	0.764	0.678	0.697	0.661	0.742	0.73	–	–
log (Na <sub>2</sub> O / K <sub>2</sub> O)	–0.40	–0.38	–0.37	–0.67	–0.42	–0.50	–0.54	–0.56	–0.55	–0.55	–0.65	–0.57	–0.51	–	–
TiO <sub>2</sub> /Zr	12.80	21.22	13.90	21.01	11.71	22.60	17.96	17.43	18.44	26.88	20.31	17.90	18.51	–	–
Cu/Zn	0.8	0.79	0.87	0.74	0.72	0	0.82	0.53	0.73	0.63	0.81	0.7	0.68	–	–
K/Rb	134.5	141.7	147.1	131.7	144.9	144.1	132.3	131.1	138.1	141.0	125.1	132.1	137.2	–	–
Rb/Sr	0.96	1.02	0.88	1.2	0.84	1.33	1.15	1.08	1.06	1.06	1.12	1.02	1.06	0.32	0.8
Cr/Zr	11.91	12.36	8.05	8.10	5.82	7.81	12.26	13.87	0.78	8.83	11.35	15.06	9.45	–	–
Ti/Zr	7.67	12.72	8.31	12.59	7.02	13.55	10.77	10.45	11.05	16.12	12.18	10.88	10.55	–	–
DF–1	–0.47	–2.91	–1.82	–0.31	–1.1	–3.62	–0.25	–0.48	–1.30	–1.48	0.97	0.008	–	–	–
DF–2	–0.53	0.05	1.125	0.231	–0.02	0.539	0.112	–0.17	0.05	0.624	0.486	0.159	–	–	–

Notes: Total iron as Fe<sub>2</sub>O<sub>3</sub>\* and FeO=Fe<sub>2</sub>O<sub>3</sub>×0.8998, UCC=Upper Continental Crust and PASS=Post-Archean Australian Shale (TAYLOR & MCLENNAN 1985; CONDIE 1993). CIA\*=100X[Al<sub>2</sub>O<sub>3</sub>/(Al<sub>2</sub>O<sub>3</sub>+CaO\*+Na<sub>2</sub>O+K<sub>2</sub>O)], PIA\*=[(Al<sub>2</sub>O<sub>3</sub>–K<sub>2</sub>O)/(Al<sub>2</sub>O<sub>3</sub>+CaO\*+Na<sub>2</sub>O–K<sub>2</sub>O)]×100, MIA=2(CIA–50), ICV\*=[Fe<sub>2</sub>O<sub>3</sub>\*+K<sub>2</sub>O+Na<sub>2</sub>O+CaO+MgO+TiO<sub>2</sub>/Al<sub>2</sub>O<sub>3</sub>], and CIW\*=[Al<sub>2</sub>O<sub>3</sub>/(Al<sub>2</sub>O<sub>3</sub>+CaO\*+Na<sub>2</sub>O)]×100, Mn\*=log [(Mn<sub>sample</sub>/Mn<sub>shale</sub>)/(Fe<sub>sample</sub>/Fe<sub>shale</sub>)], Discriminant function (DF–1)=–1.773TiO<sub>2</sub>+0.607 Al<sub>2</sub>O<sub>3</sub>+0.76Fe<sub>2</sub>O<sub>3</sub>\*–1.5MgO+0.616CaO+0.509 Na<sub>2</sub>O–1.224K<sub>2</sub>O–9.09 and Discriminant function (DF–2)=0.445TiO<sub>2</sub>+0.07Al<sub>2</sub>O<sub>3</sub>–0.25Fe<sub>2</sub>O<sub>3</sub>\*–1.142MgO+ 0.438 CaO +1.475Na<sub>2</sub>O+1.426K<sub>2</sub>O–6.861 (after ROSER & KORSCH 1988).

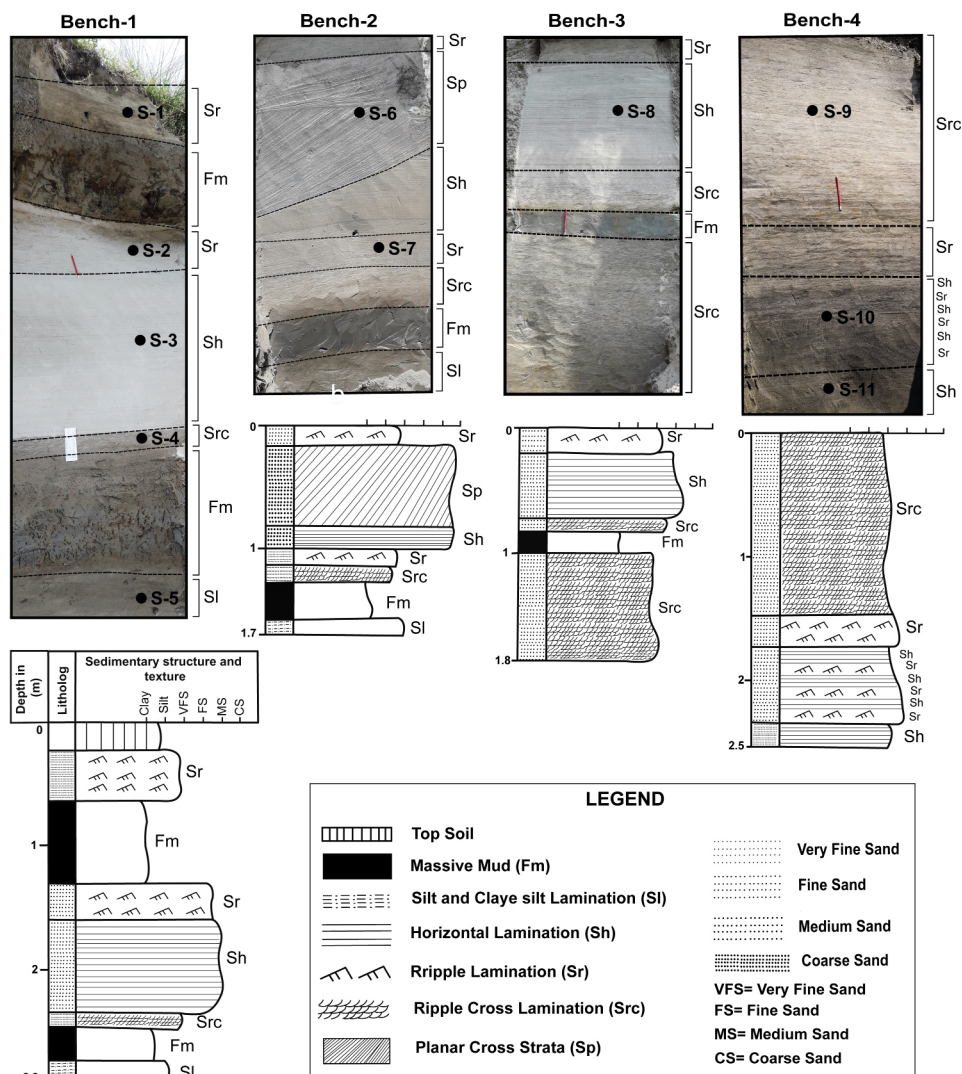


Fig. 3. Vertical lithosequences of the erosional right bank of mid channel bar of the Padma River, Rajshahi, Bangladesh. Sample points of the representative samples (viz. S-1, S-2, S-3.....S-11) for geochemical analysis are shown in the section.

### Major Elements Concentration

In accordance with the lithosuccession of the investigated area, the entire compositions of the sediments exhibit relatively wide variations in fine to medium grained sand, specifically  $\text{SiO}_2$  ranges from 59.24 wt.% (sample S-4) to 73.44 wt.% (sample S-2) with an average of 66.30 wt.% and  $\text{Al}_2\text{O}_3$  ranges from 10.39 wt.% (sample S-2) to 15.25 wt.% (sample S-5) with an average of 12.41 wt.%. These

high percentages of  $\text{SiO}_2$  and  $\text{Al}_2\text{O}_3$  demonstrate a high extent of quartz and aluminosilicates respectively. In addition, the results show low concentration of  $\text{SiO}_2$  (59.24 wt.%) and high concentration of  $\text{Al}_2\text{O}_3$  (15.25 wt.%), which demonstrates the predominance of aluminosilicate minerals. On the contrary,  $\text{SiO}_2$  exhibits high concentration (73.44 wt.%) where  $\text{Al}_2\text{O}_3$  shows low concentration (10.39 wt.%), which reveals that the dominant mineral is quartz.

Some samples are also characterized by relatively high  $\text{Fe}_2\text{O}_3$  (4.37–8.60 wt.%),  $\text{K}_2\text{O}$  (3.21–4.45 wt.%) and  $\text{CaO}$  (3.71–6.57 wt.%) contents. The average value of  $\text{Fe}_2\text{O}_3^*$  is 6.76 wt.% which is comparatively high that indicates the presence of Fe-rich minerals. The considerably high content of  $\text{CaO}$  (avg. 5.76 wt.%) of the sediments suggest that these were derived from plagioclase rich intermediate rocks with some contributions from carbonate minerals. Again,  $\text{TiO}_2$  ranges from 0.46 wt.% to 0.95 wt.% which reveals that the presence of valuable titanium-rich heavy minerals such as ilmenite and rutile. Other oxides of  $\text{ZrO}_2$  (0.036 to 0.099 wt.%) and  $\text{P}_2\text{O}_5$  (0.12 to 0.23 wt.%) may be considered diagnostic of the valuable heavy minerals zircon and monazite, respectively.

In the vertical lithosuccession of the study area, the concentration of  $\text{SiO}_2$  varies with depth. Again the average weight percentage of  $\text{SiO}_2$  (66.30 wt.%) in the studied sediments is presumably near to the mean value (66 wt.%) for the Upper Continental Crust (UCC) (TAYLOR & MCLENNAN 1985; MCLENNAN 2001; RUDNICK & GAO 2003). When the correlation coefficient ( $r$ ) is nearly 1, above 0.75, between 0.45 and 0.75 and below 0.45, it considers strong, relatively strong, moderate and weak correlation. The major oxides, such as  $\text{Al}_2\text{O}_3$ ,  $\text{TiO}_2$ ,  $\text{Fe}_2\text{O}_3$ , show strong linear negative correlation with  $\text{SiO}_2$  (i.e.,  $r=-0.90$ ) (Fig. 5a) due to the increase in mineralogical maturity (BHATIA 1983; VĎAČNÝ *et al.* 2013).  $\text{MgO}$ ,  $\text{CaO}$ ,  $\text{K}_2\text{O}$  and  $\text{P}_2\text{O}_5$  display relatively strong, moderate and weak negative correlation with  $\text{SiO}_2$ . Only  $\text{Na}_2\text{O}$  shows positive moderate correlation with  $\text{SiO}_2$  (Fig. 5a). These trends are remarkably significant and the mineralogical maturity of the studied sediments is characterized by a raise in the quartz content and reduces in unstable detrital grains, which also reflect a stratigraphic trend (VĎAČNÝ *et al.* 2013).

However,  $\text{MgO}$  and  $\text{K}_2\text{O}$  exhibit strong linear positive correlations with  $\text{Al}_2\text{O}_3$  (Fig. 5b), which suggest major influences of hydraulic fractionation according to ROY & ROSER (2012) and HOSSAIN *et al.* (2014). Again  $\text{Fe}_2\text{O}_3$  and  $\text{TiO}_2$  show moderate positive correlation and  $\text{P}_2\text{O}_5$  exhibit very weak positive correlation with  $\text{Al}_2\text{O}_3$ . On the other hand,  $\text{Na}_2\text{O}$  shows moderate negative correlation with  $\text{Al}_2\text{O}_3$ . The content of  $\text{CaO}$  is comparatively high ranges from 3.71-6.57 wt.% that indicates the presence of plagioclase with some carbonate minerals. Again, Sr shows positive correlation with  $\text{Al}_2\text{O}_3$  (Fig. 6), which may be associated with feldspar since it is a common substitute for Ca in plagioclase. The average weight percentage of  $\text{CaO}$  (5.76 wt.%) contents is enriched with the UCC value (4.20 wt.%) and almost higher than that of the

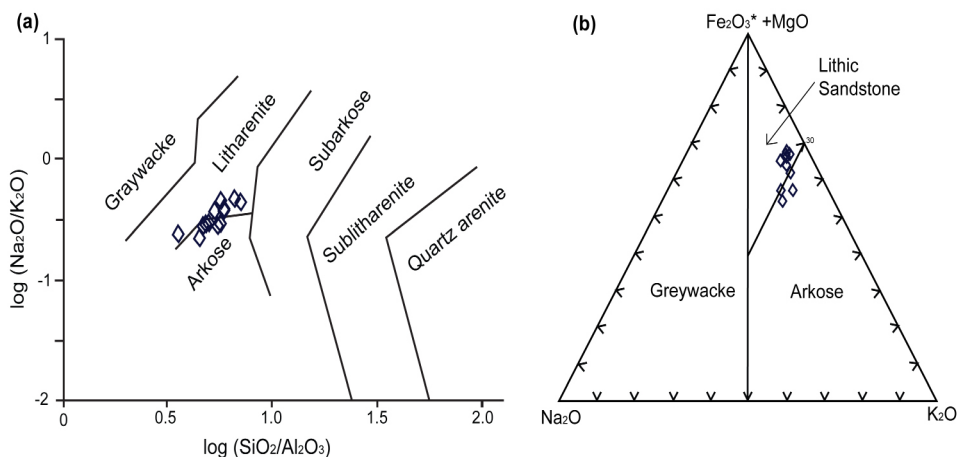


Fig. 4. (a) Plot of the investigated sediments for geochemical classification diagrams;  $\log (\text{Na}_2\text{O}/\text{K}_2\text{O})$  vs.  $\log (\text{SiO}_2/\text{Al}_2\text{O}_3)$  diagram (After PETTJOHN *et al.* 1972). (b)  $(\text{Fe}_2\text{O}_3^* + \text{MgO})$ - $\text{Na}_2\text{O}$ - $\text{K}_2\text{O}$  classification diagram for the investigated sediments (After BLATT *et al.* 1980).

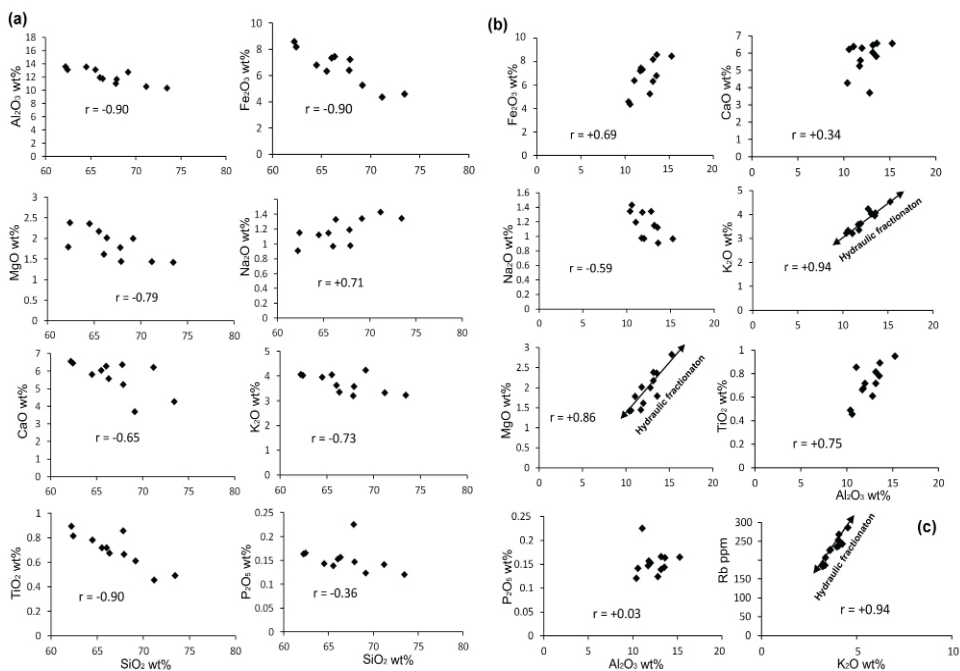


Fig. 5. Harker major element variations (in wt.%) diagram for the investigated sediments of the study area. (a) Plots of  $\text{SiO}_2$  wt.% vs. different oxides; (b) Plots of  $\text{Al}_2\text{O}_3$  wt.% vs. different oxides; and (c) Plots of  $\text{K}_2\text{O}$  wt.% vs.  $\text{Rb}$ .

Post Archean Australian Shales (PAAS) value of 1.3 wt.% (TAYLOR & MCLENNAN 1985).

The correlation coefficient between  $\text{Al}_2\text{O}_3$  and  $\text{K}_2\text{O}$  is relatively higher ( $r = +0.94$ ) than the other major oxides that suggests k-feldspar control on the major element composition of the sediments. The positive correlation between Rb and  $\text{K}_2\text{O}$  ( $r = +0.94$ ) displays hydraulic fractionation (Fig. 5c). The average value of  $\text{K}_2\text{O}$  is 3.77 wt.% which is slightly enriched compared to the UCC value (3.4 wt.%) and PAAS value (3.7 wt.%) of CONDIE (1993); TAYLOR & MCLENNAN (1985). While the average contents of  $\text{Na}_2\text{O}$  (1.16 wt.%) is depleted in accordance to the UCC value (3.9 wt.%) and mostly close to the PASS value (1.2 wt.%).

The ratio of  $\text{SiO}_2/\text{Al}_2\text{O}_3$  ranges from 3.88 to 7.07 reflects the presence of quartz as well as the feldspar content (POTTER 1978) (Table 1). The ratio of  $\text{Na}_2\text{O}/\text{K}_2\text{O}$  (0.21-0.42) of sediments is comparatively low, indicating the low degree of maturation of the sediments (PETTIJOHN *et al.* 1972; ROSER & KORSCH 1986; FEDO *et al.* 1995; PAIKARAY *et al.* 2008).  $\text{TiO}_2$  shows higher value (0.72 wt.%) than the UCC value of 0.5 wt.% (TAYLOR & MCLENNAN 1985; CONDIE 1993), which suggests more evolved with mafic and ultramafic crystalline material in the source rocks. Most of the studied samples have low  $\text{P}_2\text{O}_5$  (avg. 0.15 wt.%) contents, explaining the lesser amount of accessory phases such as apatite and monazite compared with UCC (CONDIE 1993).

#### Trace Elements Concentration

There are different kinds of trace elements found in the sediment samples of the investigated area for example, Large Ion Lithophile Elements (LILE), High Field Strength Elements (HFSE) and Transition Trace Elements (TTE). LILEs are relatively mobile and incompatible elements. The average concentrations of the LILE, like Rb (229 ppm) and Ba (630 ppm) are higher than average Upper Crustal Compositions (UCC) and Sr (216 ppm) is lower than average UCC (TAYLOR & MCLENNAN 1981) as shown in Table 1. Rb exhibits relatively strong linear positive correlation ( $r = +0.74$ ) with  $\text{Al}_2\text{O}_3$  (Fig. 6) and strong linear positive correlation ( $r = +0.94$ ) with  $\text{K}_2\text{O}$  (Fig. 5c) confirming clear hydraulic fractionation (ROY & ROSER 2012; HOSSAIN *et al.* 2014). Sr and Ba display a moderate positive correlation with  $\text{Al}_2\text{O}_3$ . Strong positive correlations of mobile components recommend their relationship with finer particles denoted the hydraulic partition of quartz and clays. HFSEs are incompatible but immobile elements. They are enriched in felsic instead of mafic rocks (BAULUZ *et al.* 2000). Due to their immobile nature, they are regarded as provenance indicators (TAYLOR & MCLENNAN 1985). The concentration of Zr is mainly controlled by the heavy mineral zircon. The average concentrations of Zr (409 ppm), and Y (111 ppm) of the sediments are enriched compared to the average UCC value (Table 1). Controlling phases for Y abundance are probably rutile and monazite because of relatively strong positive correlations with  $\text{TiO}_2$  ( $r = +0.79$ ). The TTE like Cr and Ni have much higher concentrations range of (331-6288) ppm and (74-326) ppm than UCC (CONDIE, 1993) and PAAS (TAYLOR & MCLENNAN 1985) values but have lower concentration of Cu

(0-86) ppm (Table 1). The average concentration of the other trace elements are Mn (721 ppm), Zn (84 ppm), Cl (435 ppm), F (320 ppm), S (81 ppm) and As (14 ppm).

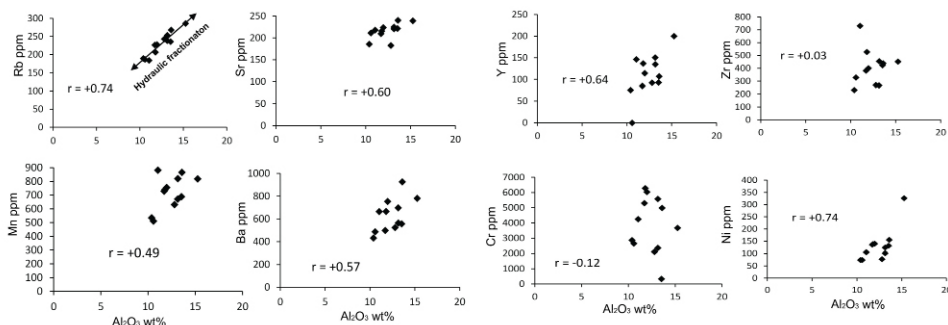


Fig. 6. Harker trace element variations (in ppm) diagram for the investigated sediments of the study area.

The UCC normalized major and trace element concentrations are showed in Fig. 7. In comparison with UCC (TAYLOR & MCLENNAN 1985), the studied recent sediments are often enriched and depleted of the major and trace elements (Table 1). The Multi-element normalized diagram exhibits enrichment of  $\text{SiO}_2$ ,  $\text{TiO}_2$ ,  $\text{Fe}_2\text{O}_3$ ,  $\text{CaO}$ ,  $\text{K}_2\text{O}$ , Ba, Rb, Zr and depletion of  $\text{Al}_2\text{O}_3$ ,  $\text{MgO}$ ,  $\text{Na}_2\text{O}$ ,  $\text{P}_2\text{O}_5$ , Sr, Ni, Cr and Y. These normalized elemental distributions indicate that the chemical weathering led to removal of the soluble elements from the clastic fractions compared to the insoluble hydrolysates (NAGARAJAN *et al.* 2013). The comparative depletion or enrichment of various elements is broadly appropriate for provenance characteristics and weathering conditions (ETEMAD-SAEED *et al.* 2011). Moreover, the higher concentration of trace elements is probably due to the influence of heavy minerals presence as well as by the nature of source rock.

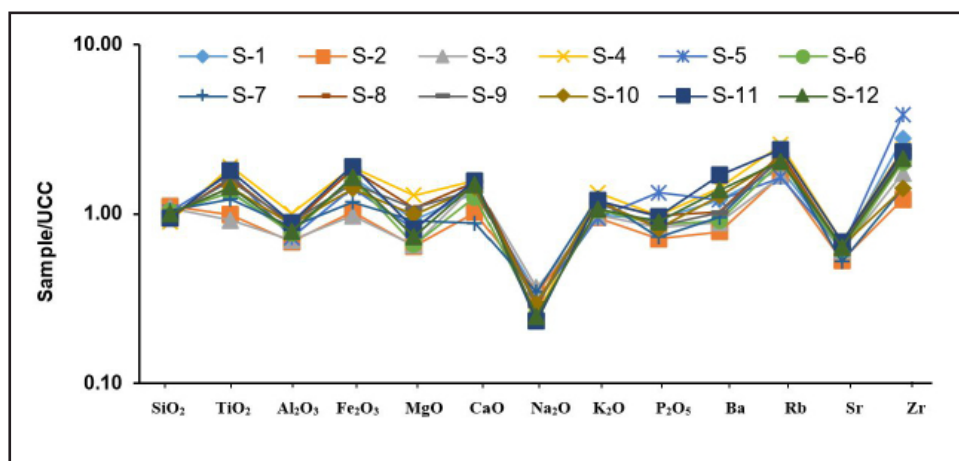


Fig. 7. Multi-element normalized diagram for the investigated sediment, normalized major and trace element against average UCC (Upper Continental Crust) values (After TAYLOR & MCLENNAN 1985).

### Geochemical Classification

Based on geochemical compositions, numerous authors have proposed a few classifications for clastic sedimentary rocks or sediments although the geochemical classification of sediments is not well developed (e.g. PETTIJOHN *et al.* 1972; CROOK 1974; HERRON 1988; BLATT *et al.* 1980). The  $\text{SiO}_2$  content and the  $\text{SiO}_2/\text{Al}_2\text{O}_3$  proportion are the most usually utilized geochemical criteria for outlining the sediment maturity (POTTER 1978). They also reflect the abundance of quartz, feldspar and clay contents in the sediments. For the index of chemical maturity, the alkali content ( $\text{Na}_2\text{O}+\text{K}_2\text{O}$ ) is appropriate for which quantifies the content of feldspar. PETTIJOHN *et al.* (1972) proposed a classification for Terrigenous sedimentary rocks dependent on a plot of  $\log (\text{Na}_2\text{O}/\text{K}_2\text{O})$  vs.  $\log (\text{SiO}_2/\text{Al}_2\text{O}_3)$  utilizing the ( $\text{Na}_2\text{O}/\text{K}_2\text{O}$ ) ratio and index of chemical maturity. On the basis of this scheme, the studied sediments show arkosic and litharenitic in composition (Fig. 4a). It is very noticeable that  $(\text{Fe}_2\text{O}_3^*+\text{MgO})-\text{Na}_2\text{O}-\text{K}_2\text{O}$  ternary diagram (BLATT *et al.* 1980) exhibits lithic with some arkose of the studied sediments (Fig. 4b). While, the applicability of the  $\text{K}_2\text{O}$  vs.  $\text{Na}_2\text{O}$  figure (CROOK 1974) for the studied sediments, it is enough to observe their quartz-rich characteristics (Fig. 10a).

### Source Area Weathering

Weathering is the process which involves the physical disintegration and chemical decomposition of the older rocks to create solid particulate residue and dissolved chemical substance. The most useful tools for characterizing and determining the extent of weathering are identification of mechanism of weathering processes, degree of weathering or various chemical weathering indices. The extent of chemical weathering of the source territory materials can be obliged by computing the Chemical Index of Alteration (CIA) (NESBITT & YOUNG 1982). The determined CIA\* values ranges from 50.12 to 59.03 (avg. 54.94) in the studied sediments which is lower than the average UCC value (Table 1). The CIA values range from (50-60), (60-80) and >80 indicate incipient, intermediate and extreme weathering respectively. The CIA\* values ranges (50-60) of the sediments studied indicates poor/incipient weathering conditions in the source area. This low value of CIA is also supported by Plagioclase Index of Alteration (PIA\*) (50.18-64.84, avg. 57.42) and Index of Compositional Variability (ICV) (1.34-1.80, avg. 1.62) values (NESBITT & YOUNG 1982; FEDO *et al.* 1995). Again high PIA value (>84) shows severe chemical weathering while lower value (~50) displays unweathered or fresh rock samples. The obtained average PIA values 57.42 exhibits relatively unweathered rock sources. The Mineralogical Index of Alteration (MIA) is another weathering parameter determined as:  $\text{MIA} = 2(\text{CIA}-50)$ . MIA values between 0-20% are named as incipient, i.e. just starting; 20-40% (weak); 40-60% (moderate) and 60-100% as intense to extreme degree of weathering respectively. The extreme value of 100% show the total weathering of a primary material into its equivalent weathered. The calculated

MIA value ranges from 0.24% to 18.06% (Avg. 9.89%), which indicates incipient weathering condition of the source material. Because minerals show resistance to weathering, ICV can be utilized as a measure of sediment maturity.

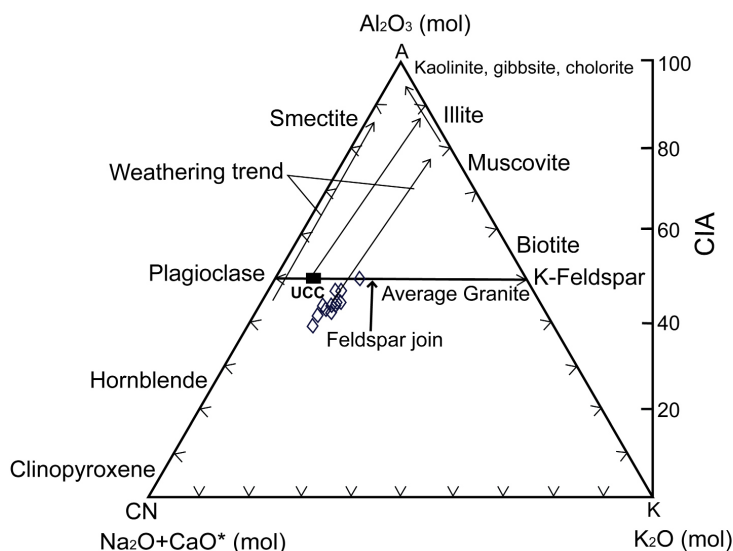


Fig. 8. Ternary plots of major element compositions of sediment samples plotted as molar proportions on an  $\text{Al}_2\text{O}_3$ –( $\text{CaO}^* + \text{Na}_2\text{O}$ )– $\text{K}_2\text{O}$  or (A–CN–K) diagram (NESBITT & YOUNG 1997). Arrow indicate the weathering trend of the sediments, the scale showing the chemical index of alteration (CIA) is shown at the right side.

The ICV value  $>1$  indicates immature sediments, while ICV values  $<1$  exhibits matured sediments. The average ICV of the studied sediment is 1.62, which represents immature sediments. Chemical Index of Weathering (CIW) is an improved measure of the degree of weathering experience by a material comparative to its parent rock. The CIW values ranges from 50 to 60 show incipient weathering, 60 to 80 exhibits intermediate weathering, and above 80 demonstrate extreme weathering. The determined values of CIW of the samples range from 59.52 to 73.40 (avg. 65.95), which reflects incipient weathering.

A useful way to evaluate the chemical weathering trend is A–CN–K molecular proportion ternary diagram which represents the plot of  $\text{Al}_2\text{O}_3$ –( $\text{CaO}^* + \text{Na}_2\text{O}$ )– $\text{K}_2\text{O}$  (NESBITT & YOUNG 1997). In the plots, most of the samples are near to the plagioclase and K-feldspar tie lines and below the UCC, indicating very poor weathering conditions or albitic-rich sources with less K mobility. The degrees of weathering are fairly different all through the succession (Fig. 8), demonstrating non steady-state

weathering conditions in the source area most likely because of increases in the intensity of tectonic activity throughout the certain timeframes, which permits rapid erosion of source rocks (NESBITT *et al.* 1997). The  $K_2O/Na_2O$  proportions range from 2.32 to 4.69 (avg. 3.35) which are  $>1$  showing quartz enrichment in the sediments. The major elements, particularly the high content of  $SiO_2$  (avg. 66.30 wt.%) also reflects quartz dominance in sediments and the variation in  $Al_2O_3$  content (10.39–5.25 wt.%) shows feldspar input instead of clay minerals that are practically missing in the samples. In this case most of the weathering indices suggest poor weathering. In addition, the ratios of Rb/Sr also monitor the degree of source-rock weathering (MCLENNAN *et al.* 1993). The average value of the proportion of Rb/Sr of the studied sediments is 1.06 which is higher than the average upper continental crust (0.32) and near to the average PAAS (0.80) (Table 1). Therefore, all these data suggest that the degree of source area weathering was most likely poor weathering conditions.

### Sorting and Sediment Recycling

The degree of sorting is controlled by the energy of the transport system, the source to sink distance, and many other factors (DOKUZ & TANYOLU 2006; ROY & ROSER 2012). Basically sorting produces geochemical contrasts among sand, silt and clay because of the detachment of these grains by hydraulic fractionation. By Harker variation diagrams, the evaluation of sorting effects and their degrees are so much helpful on such sediments. The major oxides  $Fe_2O_3$ ,  $Na_2O$ ,  $CaO$  and  $P_2O_5$  display poor linear trends with  $Al_2O_3$ , (Fig. 5b) except  $K_2O$  ( $r = +0.94$ ) and  $MgO$  ( $r = +0.86$ ) indicating significant positive trends clarifying the degree of fractionation through mineral sorting. The average ICV value of the studied sediment is 1.62 ( $>1$ ) which indicates compositionally immature to moderately mature sediments and these sediments are likely dominated by first cycle input (CULLERS & PODKOYVROV 2000).  $15*Al_2O_3-Zr-300*TiO_2$  ternary diagram (Fig. 9) exhibits the impact of sorting processes (GARCIA *et al.* 1994). This gives information on the zircon concentration in sediments with a limited range of  $TiO_2-Zr$ , demonstrating insignificant sorting of the sediments and low compositional maturity. It is suggested that the studied sediments support a limited range of  $TiO_2/Zr$  variety and a reasonable sorting trend, and those comprising of sand-size components are immature indicating poor to moderate sorting and deposition without recycling. With an increasing in  $SiO_2/Al_2O_3$  (3.88–7.07) proportion, the grain size likewise increases, as do the degree of recycling and maturity of sediment (Table 1).

### Provenance

Inorganic geochemical data and their various applications are important for provenance studies (e.g. TAYLOR & MCLENNAN 1985; CONDIE *et al.* 1992; CULLERS 1995; ARMSTRONG-ALTRIN *et al.* 2004; KESKIN 2011). Accordingly MCLENNAN *et al.*

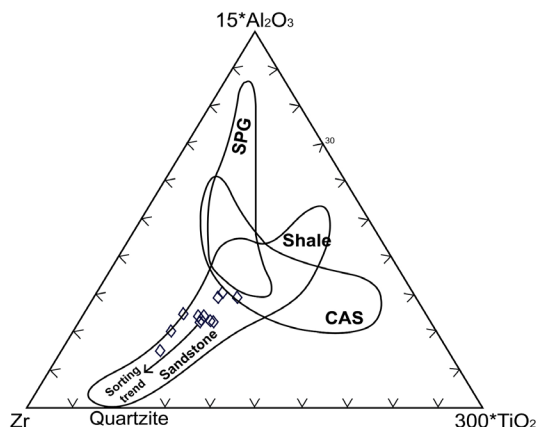


Fig. 9. Ternary plot of  $15 \cdot \text{Al}_2\text{O}_3$ -Zr- $300 \cdot \text{TiO}_2$  for the investigated sediments, CAS = field of calc-alkaline granites; SPG = field of strongly peraluminous granites (after GARCIA *et al.* 1994).

(1993) suggested that major elements give information on both the rock composition of the provenance and the impact of sedimentary processes, for example, weathering and sorting. These also depict the attribute of the source rocks and lastly give definite styles of sedimentary history (DICKINSON 1985, 1988).

It is noticeable that the ratios of  $\text{SiO}_2/\text{Al}_2\text{O}_3$  (avg. 5.44) and  $\text{K}_2\text{O}/\text{Na}_2\text{O}$  (avg. 3.35) are higher than those ratios of UCC (TAYLOR & MCLENNAN 1985; CONDIE 1993), which indicate the studied sediments were originated largely from felsic sources (Table 1). Again, the  $\text{Al}_2\text{O}_3/\text{TiO}_2$  ratio ranges from 12.89 to 23.14 with an average of 17.72, pointing out that the investigated sediments are derived from mostly felsic to intermediate rock sources (HAYASHI *et al.* 1997; KESKIN 2011 and references therein). The bivariate plot of  $\text{K}_2\text{O}$  vs.  $\text{Na}_2\text{O}$  (CROOK 1974) shows that all the samples are quartz-rich, which indicate the predominant of felsic origin (Fig. 10a).

The provenance discriminant function plot of ROSER & KORSCH (1988) characterized four (4) main provenances: mafic igneous provenance; intermediate igneous provenance; felsic igneous provenance; and quartzose sedimentary provenance (Fig. 10b). The samples plotted mainly in the felsic igneous and few quartzose sedimentary zones that are comparable fields with the quartzose sedimentary rocks in Bangladesh (HOSSAIN *et al.* 2014), however the studied recent sediments also fall in the Tertiary sedimentary rocks but maintain far distance from Siwalik deposits (Fig. 10b). Accordingly ROSER & KORSCH (1988), sediments recycled from felsic sources plot dynamically away from the igneous source line into the quartzose field. The concentration of zircon is utilized to characterize the composition and nature of source rock (HAYASHI *et al.* 1997; PAIKARAY *et al.* 2008). HAYASHI *et al.* (1997) suggest that the  $\text{TiO}_2/\text{Zr}$  ratios are great amount of supportive to recognize among three various types of source rock, i.e., felsic, intermediate and mafic. The

proportion of  $\text{TiO}_2/\text{Zr}$  ranges from 12 to 27 with an average of 19 shows that all the stream sediments are in the felsic zone. The studied sediments include relatively high  $\text{K}_2\text{O}$  and Rb concentrations (Fig. 11a) and their K/Rb ratios of approximately (126-148) with an average of 137 (Table 1), which lie near to the principal trend with a ratio of 230 of a typical differentiated magmatic suite after SHAW (1968), indicating chemically coherent nature of the sediments and mode of formation mainly from acidic to intermediate rocks.

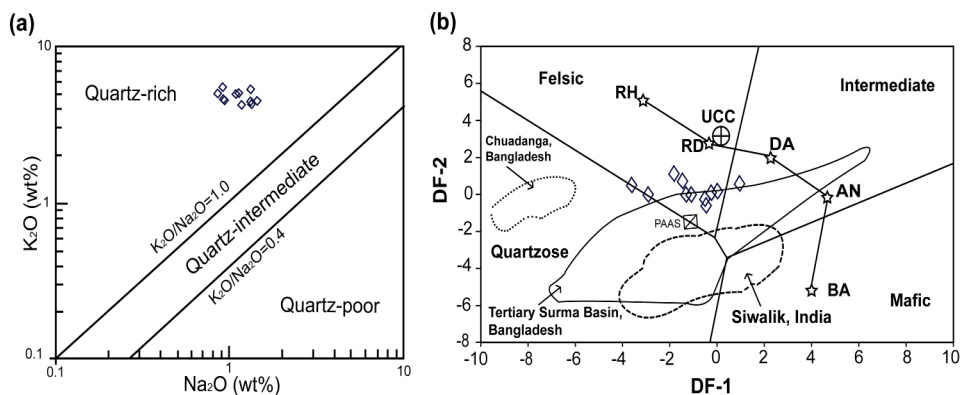


Fig. 10. (a) Bivariate plot of  $\text{K}_2\text{O}$  versus  $\text{Na}_2\text{O}$  of the studied sediments showing quartz rich nature, (after CROOK 1974). (b) Major element provenance discriminant plot (ROSER & KORSCH 1988), where fields for Siwalik, India from data in RANJAN & BANERJEE (2009), Tertiary Sedimentary Rocks, Surma Basin from HOSSAIN *et al.* (2010), Hatia trough from ROY & ROSER (2012), Quartzose Sedimentary Rocks in Chudanga District, Bangladesh (HOSSAIN *et al.* 2014), UCC and PAAS from TAYLOR & MCLENNAN (1985). Star sign indicate average value i.e. BA=Basalt, AN=Andesite, DA=Dacite, RD=Rhyodacite, RH=Rhyolite as plotted by ROSER & KORSCH (1988).

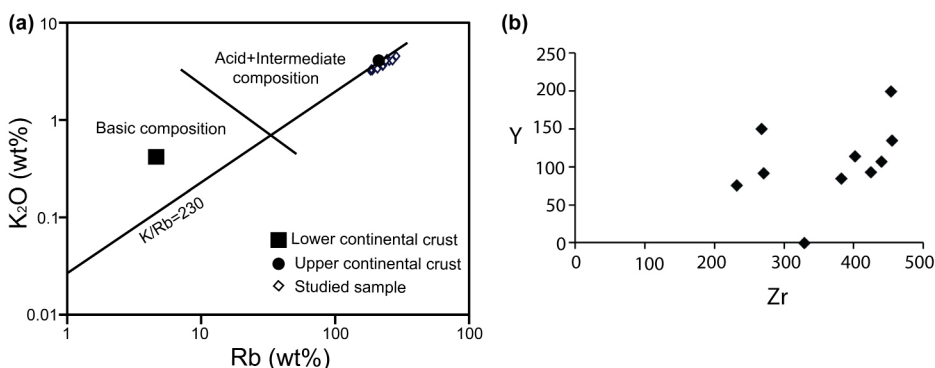


Fig. 11. (a)  $\text{K}_2\text{O}$  vs. Rb plot for the recent sediments from mid channel sand bar of the Padma River, Rajshahi, Bangladesh (After HAYASHI *et al.* 1997). (b) Harker plots showing the relations between Y and Zr trace element concentration (ppm) for the investigated sediments of the study area.

Though felsic source rocks contain relatively high Cr and Ni, some heavy mineral concentrations make uncertainty, such as Cr (331-6288) ppm with an average of

3869 ppm concentration (Table 1) of sediments are exceptionally high because of the high concentrations of chromium spinel, chromite and magnetite or significant ophiolitic component (NAGARAJAN *et al.* 2013). Usually those trace elements are necessary for the indicators of mafic and ultramafic source (WRONKIEWICZ & CONDIE 1987; HUNTSMAN–MAPILA *et al.* 2005). The studied sediments have moderate concentrations of Ba (432-928) ppm, Sr (183-240) ppm, Ni (74-326) ppm, Y (0-200) ppm and Zr (232-731) ppm. If zircons are concentrated by hydraulic sorting in the sedimentary process, the Cr/Zr ratio is expected to decrease (TAYLOR & MCLENNAN 1985; SPALLETI *et al.* 2008) (Table 1). The investigated sediments exhibit a wide range of Cr/Zr ratios (0.78-15.06), which are very much similar to the value of the originating from a mafic to felsic sources. Y displays remarkably scatter correlation with Zr (Fig. 11b), indicating a minor impact of zircon and other REE-rich heavy minerals, perhaps because it is controlled to a great extent by irregular distribution during sedimentation (LOPEZ *et al.* 2005).

### Tectonic Setting

Several geochemical classification schemes have been proposed to discriminate from the various origin and tectonic settings (BHATIA 1986; ROSER & KORSCH 1986, 1988). Sedimentary rocks have various geochemical characteristics from different tectonic settings (BHATIA 1983; ROSER & KORSCH 1986). Major and trace elements and their distinctive bivariate and multivariate plots with discrimination functions are generally suitable for tectonic setting of the sedimentary basins. Despite the fact that these applications are not constantly legitimate for explicit nearby plate-tectonic settings, for example, back-arc basin, a few correlations between geochemical composition and tectonic settings of sediments could be established and the relationships among temporal and spatial variations inside different lithostratigraphic units, can be assessed. The plot of  $(K_2O/Na_2O)$  vs.  $SiO_2$  (Fig. 12a) gives the tectonic setting discrimination for the studied Recent sediments after ROSER & KORSCH (1986). Most of the data of the studied samples shows Passive Margin (PM) to Active Continental Margin (ACM) tectonic setting. In such a setting, the sediments are quartz rich, which are originated from plate interior or stable continental areas and finally deposited in intra-cratonic basins or passive continental margins (ROSER & KORSCH 1986). BHATIA (1983) characterized  $SiO_2/Al_2O_3$  vs.  $K_2O/Na_2O$  plot (Fig. 12b) based on the chemical analysis of the clastic sediments, which demonstrates comparability to  $(K_2O/Na_2O)$  vs.  $SiO_2$  plot (Fig. 12a), where average data plot in a similar pattern. Passive margin sediments are portrayed by higher values of both ratios. ACM sediments delineate the lower  $SiO_2/Al_2O_3$  ratio with variable low  $(K_2O/Na_2O)$  ratio (MCLENNAN *et al.* 1993). On the Major element-based diagram of BHATIA (1983), the present study is plotted in the field of passive margin (PM) to active continental margin (ACM) setting.

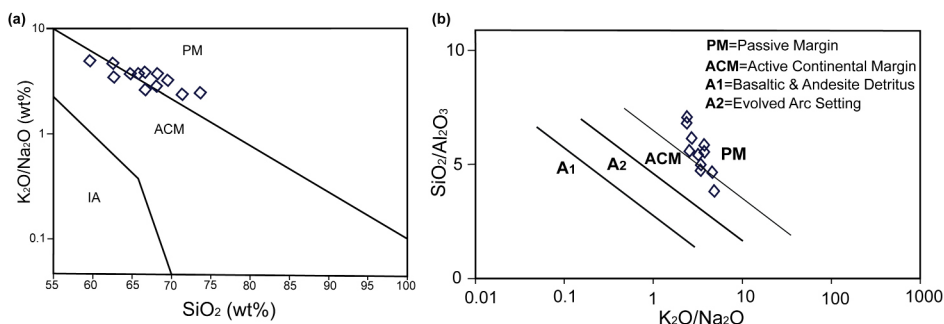


Fig. 12. (a) Tectonic setting discrimination diagram of  $(K_2O/Na_2O)$  vs.  $SiO_2$  for the investigated Recent sediments (after ROSER & KORSCH 1986). (b) Tectonic Discriminant diagram of  $SiO_2/Al_2O_3$  vs.  $K_2O/Na_2O$  for the investigated Recent sediments showing in the field of passive margin (PM) to active continental margin (ACM) (after ROSER & KORSCH 1986).

Several trace element concentrations (e.g. Ba, Rb and Y) and the ratios of Ti/Zr also demonstrate clearly tectonic setting. BHATIA & CROOK (1986) have exhibited that ocean island arc derived sediments are shown by Ti/Zr ratios generally  $>40$ , those originate from continental island arcs have Ti/Zr ratios between 10 and 35, while those derive from passive margins generally have Ti/Zr ratios  $<10$ . So the Ti/Zr ratios of the studied sediments (7–16, avg. 11) clearly indicates passive margin (Table 1). Therefore, on the basis of major and trace elements discrimination, the tectonic setting of the sediments demarcates typically passive margin to active continental margin.

## Conclusions

The investigated Recent sediments of the channel bar of the Ganges (Padma) River, Bangladesh show mostly wider variations in fine to medium grained sand of their major element geochemistry, reflecting the nonsteady-state conditions for provenance and tectonic setting. The tectonic setting discrimination plots ( $K_2O/Na_2O$  vs.  $SiO_2$  and  $SiO_2/Al_2O_3$  vs.  $K_2O/Na_2O$ ) of the sediments in the source area belong to Passive Margin (PM) to Active Continental Margin (ACM). The values of the ratio of  $SiO_2/Al_2O_3$  (3.88–7.07), CIA\* (50.12–59.03), ICV (1.62) and PIA\* (50.18–64.84) show low degrees of maturity suggesting poor/incipient chemical weathering in source areas. From the  $Al_2O_3$ –( $CaO^*+Na_2O$ )– $K_2O$  molecular proportion ternary plot, it reveals that the analyzed samples are very close to the plagioclase and K-feldspar tie lines and beneath the UCC (Upper Continental Crust), indicating very poor weathering conditions. The values of  $SiO_2/Al_2O_3$  (3.88–7.07),  $K_2O/Na_2O$  (2.32–4.69) and  $Al_2O_3/TiO_2$  (12.89–23.14) indicates that the investigated sediments are derived from mostly felsic to intermediate source rock that are present in a vast region of the Himalayan belt as well as catchment areas of the Ganges River.

### Acknowledgements

This work is a part of first author's M.S. thesis at the Department of Geology and Mining, University of Rajshahi, Rajshahi, Bangladesh. The authors would like to thank the Director, Institute of Mining, Mineralogy and Metallurgy (IMMM), Joypurhat, Bangladesh for facilitating the geochemical laboratory works. Thanks are also to the Chairman, Department of Geology and Mining, University of Rajshahi, Bangladesh. The authors are also grateful to the reviewers for their anonymous constructive reviews and comments.

### References

- ABEDEN, J., RAHMAN, J.J., SAYEM, S.A. & ABDULLAH, R., 2018, Heavy mineral distribution in sand deposits from the lower reaches of the Jamuna River, Bangladesh; *Bangladesh Geoscience Journal*, **24**, 1–15.
- ALAM, M., 1989, Geology and depositional history of Cenozoic sediments of the Bengal Basin of Bangladesh; *Paleogeography Paleoclimatology Paleoecology*, **69**, 125–139.
- ALAM, M.M., 1992, Sedimentology of large braided fluvial system: The Jamuna River Bangladesh; *Bangladesh Journal of Scientific Research*, **10** (1), 79–88.
- ALLISON, M.A., 1998, Historical changes in the Ganges–Brahmaputra delta front; *Journal of Coastal Research*, **14**, 1269–1275.
- ARMSTRONG–ALTRIN, J.S., LEE, Y.I., VERMA, S.P. & RAMASAMY, S., 2004, Geochemistry of sandstones from the Upper Miocene Kudankulam Formation, southern India: Implications for provenance, weathering, and tectonic setting; *Journal of Sedimentary Research*, **74**, 285–297.
- BASU, A., 1985, Influence of climatic and relief on compositions of sands released at source areas; In: ZUFFA G.G. (ed.) *Provenance of arenites*: NATO, Advanced Study Institute series, 1–18.
- BAULUZ, B., MAYAYO, M.J., FERNANDEZ–NIETO, C. & LOPEZ, J.M.G., 2000, Geochemistry of Precambrian and Paleozoic siliciclastic rocks from the Iberian Range (NE Spain): implications for source–area weathering, sorting, provenance, and tectonic setting; *Chemical Geology*, **168**, 135–150.
- BHATIA, M.R., 1983, Plate tectonics and geochemical composition of sandstones; *J. Geol.* **91**, 611–627.
- BHATIA, M.R. & CROOK, K.A.W., 1986, Trace element characteristics of graywackes and tectonic setting discrimination of sedimentary basin; *Contributions to Mineralogy and Petrology*, **92**, 181–193.
- BHATT, M.I. & GHOSH, S.K. 2001, Geochemistry of 2.51 Ga old Rampur Group pelites, western Himalayas: Implications from their provenance and weathering; *Precambrian Research*, **108**, 1–16.
- BLATT, H., MIDDLETON, G.D. & MURRAY, R., 1980, *Origin of Sedimentary Rocks*; 2nd edition, Prentice–Hall, New Jersey, 782p.
- CONDIE, K.C., NOLL, P.D. & CONWAY, C.M., 1992, Geochemical and detrital mode evidence for two sources of Early Proterozoic metasedimentary rocks from the Tonto Basin Supergroup, central Arizona; *Sedimentary Geology*, **77**, 51–76.
- CONDIE, K.C., 1993, Chemical composition and evolution of the upper continental crust: Contrasting results from surface samples and shales; *Chemical Geology*, **104**, 1–37.
- CROOK, K.A.W., 1974, Lithogenesis and geotectonics: The significance of compositional variation in flyscharenites (greywackes); *Society of Economical, Paleontological and Mineralogical Special Publications*, **19**, 304–310.
- CULLERS, R.L., 1995, The controls on the major and trace element evolution of shales, siltstones and sandstones of Ordovician to Tertiary age in the Wet Mountain region, Colorado, U.S.A.; *Chemical Geology*, **123**, 107–131.

- CULLERS, R.L. & PODKOYVROV, V.N., 2000, Geochemistry of the Mesoproterozoic Lakhanda shales in southeastern Yakutia, Russia: Implications for mineralogical and provenance control, and *recycling*; *Precambrian Research*, **104**, 77–93.
- DICKINSON, W.R., BEARD, L.S., BRAKENRIDGE, G.R., ERJAVEC, J.L., FERGUSON, R.C., INMAN, K.F., KNEPP, R.A., LINDBERG, F.A. & RYBERG, P.T., 1983, Provenance of North American Phanerozoic sandstones in relation to tectonic setting; *Geological Society of America Bulletin*, **94**, 222–235.
- DICKINSON, W.R., 1985, Interpreting provenance relations from detrital modes of sandstones; In: ZUFFA G.G. (ed.) *Provenance of Arenites Dordrecht–Boston–Lancaster*. D. Reidel Pub. Co., 333–361.
- DICKINSON, W.R., 1988, Provenance and sediment dispersal in relation to paleo–tectonics, and paleo–geography of sedimentary basins; In: KLEINSPEHN K.L. & PAOLA C. (eds.) *New Perspectives in Basin Analysis* New Springer Verlag, 3–25.
- DOKUZ, A. & TANYOLU, E., 2006, Geochemical constraints on the provenance, mineral sorting and subaerial weathering of Lower Jurassic and Upper Cretaceous clastic rocks of the eastern Pontides, Yusufeli (Artvin), NE Turkey; *Turkish Journal of Earth Sciences*, **15**, 181–209.
- ETEMAD-SAEED, N., HOSSEINI-BARZI, M. & ARMSTRONG-ALTRIN, J.S., 2011, Petrography and geochemistry of clastic sedimentary rocks as evidences for provenance of the Lower Cambrian Lalun Formation, Posht-e-Badam block, Central Iran; *Journal of African Earth Sciences*, **61**, 142–159.
- FEDO, C.M., NESBITT, H.W. & YOUNG, G.M., 1995, Unraveling the effects of potassium metasomatism in sedimentary rock sand paleosols, with implications for paleoweathering conditions and provenance; *Geology*, **23**, 921–924.
- GAILLARDET, J., DUPRE, B. & ALLEGRE, C.J., 1999, Geochemistry of large river suspended sediments: silicate weathering or recycling tracer? *Geochimica et Cosmochimica Acta*, **63**, 4037–4051.
- GARCIA, D., FONTEILLES, M. & MOUTTE, J., 1994, Sedimentary fractionation between Al, Ti, and Zr and genesis of strongly peraluminous granites; *Journal of Geology*, **102**, 411–422.
- GARZANTI, E., ANDO, S., FRANCE-LANORD, C., VEZZOLI, G., CENSI, P., GALY, V. & NAJMAN, Y., 2010, Mineralogical and chemical variability of fluvial sediments: 1. Bed load sand (Ganga–Brahmaputra, Bangladesh); *Earth Planetary Science Letters*, **299** (3), 368–381.
- GARZANTI, E., ANDO, S., FRANCE-LANORD, C., CENSI, P., VIGNOLA, P., GALY, V. & LUPKER, M., 2011, Mineralogical and chemical variability of fluvial sediments 2. Suspended load silt (Ganga–Brahmaputra, Bangladesh); *Earth Planetary Science Letters*, **302** (1), 107–120.
- GOTO, A. & TATSUMI, Y., 1994, Quantitative analysis of rock samples by an X-ray fluorescence spectrometer (I); *The Rigaku Journal*, **11**, 40–59.
- GOTO, A. & TATSUMI, Y., 1996, Quantitative analysis of rock samples by an X-ray fluorescence spectrometer (II); *The Rigaku Journal*, **13**, 20–38.
- HAQUE, M. M. & ROY, M. K., 2016, Petrography and Geochemistry of the Miocene Sandstone, Bandarban Anticline, Bangladesh: Implications for Provenance and Tectonic Setting; *Life and Earth Science Journal*, **11**, 43–50.
- HAYASHI, K., FUJISAWA H., HOLLAND, H.D. & OHMOTO, H., 1997, Geochemistry of 1.9 Ga sedimentary rocks from northeastern Labrador, Canada; *Geochimica et cosmochimica Acta*, **61**, 4115–4137.
- HENRY, Y. M., 2017, Source–area weathering, composition and paleo–redox condition of stream sediments from Ijero–Ekiti, Nigeria; *International Journal of Trend in Scientific Research and Development (IJTSRD)*, **1**, 746–765.
- HERRON, M.M., 1988, Geochemical classification of terrigenous sands and shales from core or log data; *Sedimentary Petrology*, **58**, 820–829.
- HOSSAIN, H.M.Z., ROSER B.P. & KIMURA J.I., 2010, Petrography and whole–rock geochemistry of the Tertiary Sylhet succession, northeastern Bengal Basin, Bangladesh: Provenance and source area weathering; *Sedimentary Geology*, **228**, 171–183.
- HOSSAIN, I., ROY, M.K., BISWAS, P.K., ALAM M., MONIRUZZAMAN, M. & DEEBA, F., 2014, Geochemical

- characteristics of Holocene sediments from Chuadanga district, Bangladesh: Implications for weathering, climate, redox conditions, provenance and tectonic setting; *China Journal of Geochemistry*, **33**, 336–350.
- HOSSAIN, M.S., KHAN, M.S.H., CHOWDHURY, K.R. & ABDULLAH, R., 2019, Synthesis of the Tectonic and Structural Elements of the Bengal Basin and Its Surroundings; In: MUKHERJEE, S. (ed.) *Tectonics & Structural Geology: Indian Context*: Springer International Publishing AG, Cham. 135–218. doi: 10.1007/978-3-319-99341\_6
- HOSSAIN, M.S., XIAO, W., KHAN, M.S.H., CHOWDHURY, K.R. & AO, S., 2020, Geodynamic model and tectono-structural framework of the Bengal Basin and its surroundings; *Journal of Maps*, **16** (2), 445–458, doi: 10.1080/17445647.2020.1770136
- HUNTSMAN–MAPILA, P., KAMPUNZU, A.B., VINK, B. & RINGROSE, S., 2005, Cryptic indicators of provenance from the geochemistry of the Okavango Delta sediments, Botswana; *Sedimentary Geology*, **174**, 123–148.
- JANNATUL, B. J., JULLEH, J. R. & RUMANA Y., 2010, Sand petrology of the exposed bar deposits of the Brahmaputra–Jamuna River, Bangladesh: Implication for Provenance; *Bangladesh Geoscience Journal*, **16**, 1–22.
- KESKIN, S., 2011, Geochemistry of Çamardı Formation sediments, central Anatolia (Turkey): Implication of source area weathering, provenance, and tectonic setting; *Geoscience Journal*, **15**, 185–195.
- KHAN, A.A., & RAHMAN T., 1992, An analysis of the gravity field and tectonic evaluation of the North western part of Bangladesh; *Tectonophysics*, **206**, 351–364.
- KHAN, F.H., 1991, *Geology of Bangladesh*, Willey Eastern limited, New Delhi, 207p.
- LOPEZ, J.M.G., BAULUZ, B., FERNANDEZ–NIETO, C. & OLIETE, A.Y., 2005, Factors controlling the trace–element distribution in fine–grained rocks: The Albian kaolinite–rich deposits of the Oliete Basin (NE Spain); *Chemical Geology*, **214**, 1–19.
- LUPKER, M., FRANCE–LANORD, C., GALLY, V., LAVE, J., GAILLARDET, J., GAJUREL, A.P., GUILMETTE, C., RAHMAN, M., SINGH S.K. & SINHA, R., 2012, Predominant floodplain over mountain weathering of Himalayan sediments (Ganga basin); *Geochimica et Cosmochimica Acta*, **84**, 410–432.
- MCLENNAN, S.M., HEMMING, S., MCDANIEL, D.K. & HANSON, G.N., 1993, Geochemical approaches to sedimentation, provenance and tectonics; *Geological Society of America*, **285**, 21–40.
- MCLENNAN, S.M., 2001, Relationships between the trace element composition of sedimentary rocks and upper continental crust; *Geochemistry Geophysics Geosystems*, **2**, 2000GC000109.
- MIALL, A.D., 1978, Lithofacies types and vertical profiles in braided river deposits: A summary; *Geological Survey of Canada*, 579–604.
- MIALL, A.D. 1978, Lithofacies summary; In: MIALL, A.D. (Ed.). *Fluvial Sedimentology*; Canadian Society of Petroleum Geologists, memoir 5, 597–604.
- NAGARAJAN, R., ROY, P.D., JONATHAN, M.P., LOZANO, R., KESSLER, F.L. & PRASANNA, M.V., 2014, Geochemistry of Neogene sedimentary rocks from Borneo Basin, East Malaysia: Paleo–weathering, provenance and tectonic setting; *Chemie Der Erde–Geochemistry*, **74**, 139–146.
- NAJMAN, Y., BICKLE, M., BOUDAGHER–FADEL, M., CARTER, A., GARZANTI, E., PAUL, M., WIJBRANS, J., WILLETT, E., OLIVER, G., PARRISH, R., AKHTER, S.H., ALLEN, R., CHISTY, E., REISBERG, L. & VEZZOLIG, 2008, The Paleogene record of Himalayan erosion: Bengal Basin, Bangladesh; *Earth and Planetary Science Letters*, **273**, 1–14.
- NESBITT, H.W. & YOUNG, G.M., 1982, Early Proterozoic climates of sandstone mudstone suites using SiO<sub>2</sub> content and K<sub>2</sub>O/Na<sub>2</sub>O ratio; *Nature*, **299**, 715–717.
- NESBITT, H.W., YOUNG, G.M., MCLENNAN, S.M. & KEAYS, R.R., 1996, Effects of chemical weathering and sorting on the petrogenesis of siliciclastic sediments, with implications for provenance studies; *Journal of Geology*, **104**, 525–542.
- NESBITT, H.W., FEDO, C.M. & YOUNG, G.G., 1997, Quartz and feldspar stability, steady and non–steady–state weathering, and petrogenesis of siliciclastic sands and muds; *Journal of Geology*, **105**, 173–191.
- PAIKARAY S., BANERJEE S., & MUKHERJI S., 2008, Geochemistry of shales from Paleoproterozoic to Neoproterozoic Vindhyan Super–group: Implications on provenance, tectonic and paleoweathering; *Journal of*

*Asia Earth Science*, **32**, 34–48.

- PETTIJOHN, F.J., POTTER, P.E. & SIEVER, R., 1972, Sand and Sandstone. Plate motions inferred from major element chemistry of lutites; *Precambrian Research*, **147**, 124–147.
- POTTER, P.E. 1978, Petrology and chemistry of big river sands, *Journal of Geology*, **86**, 423–449.
- RANJAN, N. & BANERJEE, D.M., 2009, Central Himalayan crystallines as the primary source for the sandstone–mudstone suites of the Siwalik Group: New geochemical evidence; *Gondwana Research*, **16**, 687–696.
- REIMANN, K.U., 1993, *Geology of Bangladesh*; Gebruder Borntrager, Berlin, 160p.
- ROSER, B.P. & KORSCH, R.J., 1986, Determination of tectonic setting of sandstone mudstone suites using  $\text{SiO}_2$  content and  $\text{K}_2\text{O}/\text{Na}_2\text{O}$  ratio, *Journal of Geology*, **94**, 635–650.
- ROSER, B.P. & KORSCH, R.J., 1988, Provenance signatures of sandstone–mudstone suites determined using discriminant function analysis of major–element data; *Chemical Geology*, **67**, 119–139.
- ROY, D. & ROSER, B.P., 2012, Geochemistry of the Tertiary sequence in the Shahbajpur–1 well, Hatia Trough, Bengal Basin, Bangladesh: Provenance, source weathering and province affinity; *Journal of Life and Earth Science*, **7**, 1–13.
- RUDNICK, R.L. & GAO, S., 2003, Composition of the continental crust; In: RUDNICK R.L. (ed.) *The Crust Treatise on Geochemistry* Elsevier–Pergamon, Oxford.
- RUST, B.R., 1978, Depositional models for braided alluvium In: MAILL A.D. (ed.) *Fluvial Sedimentology*, *Canadian Society of Petroleum Geologists, Memoir*, **5**, 605–626.
- SHARMA, A., SENSARMA, S., KUMAR, K., KHANNA, P.P. & SAINI, N.K., 2013, Mineralogy and geochemistry of the Mahi River sediments in tectonically active western India: implications for Deccan large igneous province source, weathering and mobility of elements in a semi–arid climate; *Geochimica et Cosmochimica Acta*, **104**, 63–83.
- SHAW, D.M., 1968, A review of K–Rb fractionation trends by covariance analysis; *Geochimica et Cosmochimica Acta*, **32**, 573–602.
- SINGH, P., 2009, Major, trace and REE geochemistry of the Ganga River sediments: influence of provenance and sedimentary processes; *Chemical Geology*, **266**, 242–255.
- SINGH, P., 2010, Geochemistry and provenance of stream sediments of the Ganga River and its major tributaries in the Himalayan region, India; *Chemical Geology*, **269** (3), 220–236.
- SINHA, S., ISLAM, R., GHOSH, S.K., KUMAR, R. & SANGODE, S.J., 2007, Geochemistry of Neogene Siwalik mudstones along Punjab re–entrant, India: Implications for source–area weathering, provenance and tectonic setting; *Current Science*, **92**, 1103–1113.
- SPALLETTI, L.A., QUERALT, I., MATHEOS, S.D., COLOMBO, F., MAGGI, J., 2008, Sedimentary petrology and geochemistry of siliciclastic rocks from the Upper Jurassic Tordillo Formation (Neuquen Basin, western Argentina): Implications for provenance and tectonic setting; *Journal of South American Earth Sciences*, **25**, 440–463.
- TAYLOR, S.R. & MCLENNAN, S.M., 1981, The composition and evolution of the continental crust: Rare earth evidence from sedimentary rocks; *Philosophical Transactions of the Royal Society of London Series A—Mathematical Physical and Engineering Sciences*, **30**, 381–399.
- TAYLOR, S.R., & MCLENNAN, S.M., 1985, *The Continental Crust: Its Composition and Evolution: An Examination of the Geochemical Record Preserved in Sedimentary Rocks*; Blackwell Scientific publication, Oxford, 312p.
- TRIPATHI, J.K., GHAZANFARI, P., RAJAMANI, V. & TANDON, S.K., 2007, Geochemistry of sediments of the Ganges alluvial plains: evidence of large–scale sediment recycling; *Journal of Quaternary International*, **159**, 119–130.
- UDDIN A. & LUNDBERG N., 1998, Unroofing history of the eastern Himalaya and the Indo–Burman ranges: heavy mineral study of Cenozoic sediments from the Bengal Basin, Bangladesh; *Journal of Sedimentary Research*, **68**, 465–472.

- VĎAČNÝ, M., VOZÁROVÁ, A. & VOZÁR, J., 2013, Geochemistry of the Permian sandstones from the Malu'íná Formation in the Malé Karpaty Mts (Hronic Unit, Western Carpathians, Slovakia): implications for source-area weathering, provenance and tectonic setting; *Geologica Carpathica*, **64** (1), 23–38.
- WRONKIEWICZ, D.J. & CONDIE, K.C., 1987, Geochemistry of Archean shales from the Witwatersrand Supergroup, South Africa: Source–area weathering and provenance; *Geochimica et Cosmochimica Acta*, **51**, 2401–2416.

*Accepted 16 July, 2020*

## বাংলাদেশের গঙ্গা (পদ্মা) নদীর চরের নব্য পললের ভূ-রাসায়নিক বৈশিষ্ট্যসমূহ

সোহাগ আলী, মোঃ শফিকুল আলম, সৈয়দ সামসুদ্দিন আহমেদ  
মোহাম্মদ নাজিম জামান, ইসমাইল হোসেন ও প্রদীপ কুমার বিশ্বাস

### সারসংক্ষেপ

বর্তমান গবেষণায় বাংলাদেশের গঙ্গা (পদ্মা) নব্য পললের ভূ-রাসায়নিক বৈশিষ্ট্য নিয়ে আলোচনা করা হয়েছে। এই গবেষণার মূল উদ্দেশ্য হলো উৎস অঞ্চলের বিচূর্নিভবন, বাছাইকরণ এবং পলির পুনর্ব্যবহারযোগ্য, উৎস শিলার উৎপত্তি এবং টেকটোনিক সেটিং বর্ণনা করা। পলির ভূ-রাসায়নিক বৈশিষ্ট্যসমূহ, তাদের প্রধান উপাদানগুলোর স্তরবিন্যাস অনুসারে তুলনামূলক বিস্তৃত ভিন্নতা প্রদর্শন করে (উদাহরণস্বরূপঃ  $\text{SiO}_2$ : 59.24–73.44,  $\text{Al}_2\text{O}_3$ : 10.39–15.25 in wt.%), যা উৎস শিলার উল্লেখযোগ্য বৈশিষ্ট্য এবং টেকটোনিক সক্রিয়তার ক্ষেত্রে একটা পরিবর্তনশীল সময়ের অংশ হিসেবে প্রতিফলিত করে। কিছু প্রধান উপাদানগুলোর অক্সাইডসমূহ (যেমন  $\text{K}_2\text{O}$ ,  $\text{TiO}_2$ , and  $\text{MgO}$ ) এবং ট্রেস উপাদানগুলো (যেমন Rb and Ni) এর সাথে বিস্তৃত সম্পর্ক প্রদর্শন করে যা তাদের সম্ভাব্য হাইড্রোলিক ভগ্নাংশ নিশ্চিত করে। অধীত পললের ভূ-রাসায়নিক শ্রেণিবিন্যাস চিত্র ইঙ্গিত করে যে, উৎস শিলা আরকোজ এবং লিথারেনাইট গোত্রের।  $\text{SiO}_2/\text{Al}_2\text{O}_3$ , CIA\*, ICV\* and PIA\* মানগুলো উৎস শিলার নিম্ন পরিপক্বতা ও উৎস শিলা অঞ্চলের নিম্ন রাসায়নিক বিচূর্নিভবন নির্দেশ করে। সমগ্র ভূ-রাসায়নিক ফলাফল থেকে প্রতীয়মান হয় যে, অধীত পললের উৎস শিলা মূলত ফেলসিক ও মধ্যবর্তী আগ্নেয় শিলা থেকে উৎপন্ন হয়েছিল। এই ধরনের শিলা হিমালয় পর্বতমালার বিস্তীর্ণ অঞ্চল সমূহে এবং গঙ্গা নদীর উৎস অঞ্চলে বিদ্যমান। অধীত পললের টেকটোনিক সেটিং বৈষম্য চিত্র সমূহ ( $\text{K}_2\text{O}/\text{Na}_2\text{O}$  vs.  $\text{SiO}_2$  এবং  $\text{SiO}_2/\text{Al}_2\text{O}_3$  vs.  $\text{K}_2\text{O}/\text{Na}_2\text{O}$ ) ইঙ্গিত করে যে, উৎস অঞ্চলের শিলা প্যাসিভ মার্জিন (PM) ও অ্যাক্টিভ কন্টিনেন্টাল মার্জিন (ACM) এর অন্তর্গত।